

# Diphenyl Ether Non-Nucleoside Reverse Transcriptase Inhibitors with Excellent Potency Against Resistant Mutant Viruses and Promising Pharmacokinetic Properties

Zachary K. Sweeney,<sup>\*[a]</sup> Joshua J. Kennedy-Smith,<sup>[a]</sup> Jeffrey Wu,<sup>[a]</sup> Nidhi Arora,<sup>[a]</sup> J. Roland Billedeau,<sup>[a]</sup> James P. Davidson,<sup>[f]</sup> Jennifer Fretland,<sup>[e]</sup> Julie Q. Hang,<sup>[d]</sup> Gabrielle M. Heilek,<sup>[c]</sup> Seth F. Harris,<sup>[b]</sup> Donald Hirschfeld,<sup>[a]</sup> Petra Inbar,<sup>[g]</sup> Hassan Javanbakht,<sup>[c]</sup> Jesper A. Jernelius,<sup>[f]</sup> Qingwu Jin,<sup>[f]</sup> Yu Li,<sup>[d]</sup> Weiling Liang,<sup>[a]</sup> Ralf Roetz,<sup>[a]</sup> Keshab Sarma,<sup>[f]</sup> Mark Smith,<sup>[a]</sup> Dimitrio Stefanidis,<sup>[g]</sup> Guoping Su,<sup>[c]</sup> Judy M. Suh,<sup>[a]</sup> Armando G. Villaseñor,<sup>[b]</sup> Michael Welch,<sup>[f]</sup> Fang-Jie Zhang,<sup>[f]</sup> and Klaus Klumpp<sup>[d]</sup>

*Non-nucleoside reverse transcriptase inhibitors (NNRTIs) are part of the preferred treatment regimens for individuals infected with HIV. These NNRTI-based regimens are efficacious, but the most popular NNRTIs have a low genetic barrier to resistance and have been associated with adverse events. There is therefore still a need for efficacious antiviral medicines that facilitate patient adherence and allow durable suppression of viral replication. As part of an extensive program targeted toward the discovery of NNRTIs that have favorable pharmacokinetic properties, good potency against NNRTI-resistant viruses, and a high genetic barrier*

*to drug resistance, we focused on the optimization of a series of diaryl ether NNRTIs. In the course of this effort, we employed molecular modeling to design a new set of NNRTIs that are active against wild-type HIV and key NNRTI-resistant mutant viruses. The structure–activity relationships observed in this series of compounds provide insight into the structural features required for NNRTIs that inhibit the replication of a wide range of mutant viruses. Selected compounds have promising pharmacokinetic profiles.*

## Introduction

Since the approval of the nucleoside AZT in 1987, 25 medicines have been introduced for the treatment of human immunodeficiency virus (HIV) infection.<sup>[1]</sup> The administration of combinations of these drugs strongly suppresses viral replication, and the amount of HIV RNA circulating in patients usually drops to undetectable levels shortly after therapy is initiated. However, the observation of detectable virus after a period of viral suppression (viral breakthrough) still occurs in an unacceptable percentage of infected individuals.<sup>[2]</sup> Analysis of the genome of the circulating virus in patients that have experienced viral breakthrough generally shows that the virus has mutated to develop resistance to one or more of the antiviral medicines.

Viral breakthrough results from inadequate inhibition of viral replication in patients treated with antiviral drugs.<sup>[3]</sup> There are a large number of infected cells in HIV patients, and the HIV virus has an inherent propensity for mutation. When replication is only partially suppressed, the virus can quickly evolve to produce mutant viruses that are resistant to the treatment regimen. Clinical studies have demonstrated that viral replication is most effectively suppressed with antiviral drugs that are potent and have pharmacokinetic characteristics that provide continuously high circulating drug levels.<sup>[4]</sup> Patient compliance is also an important determinant of antiviral treatment durability. Patients are more likely to adhere to a treatment regimen if

the drugs cause minimal side effects and can be administered once or twice daily.

[a] Dr. Z. K. Sweeney, Dr. J. J. Kennedy-Smith, J. Wu, N. Arora, J. R. Billedeau, D. Hirschfeld, W. Liang, R. Roetz, Dr. M. Smith, J. M. Suh  
Department of Medicinal Chemistry, Roche Palo Alto  
3431 Hillview Avenue, Palo Alto, CA 94304 (USA)  
Fax: (+1) 650-852-1311  
E-mail: zachary.sweeney@roche.com

[b] Dr. S. F. Harris, A. G. Villaseñor  
Department of Discovery Sciences and Technologies, Roche Palo Alto  
3431 Hillview Avenue, Palo Alto, CA 94304 (USA)

[c] Dr. G. M. Heilek, Dr. H. Javanbakht, Dr. G. Su  
Department of Viral Disease Biology, Roche Palo Alto  
3431 Hillview Avenue, Palo Alto, CA 94304 (USA)

[d] Dr. J. Q. Hang, Y. Li, Dr. K. Klumpp  
Department of Viral Disease Biochemistry, Roche Palo Alto  
3431 Hillview Avenue, Palo Alto, CA 94304 (USA)

[e] Dr. J. Fretland  
Department of Non-Clinical Safety, Roche Palo Alto  
3431 Hillview Avenue, Palo Alto, CA 94304 (USA)

[f] Dr. J. P. Davidson, Dr. J. A. Jernelius, Q. Jin, Dr. K. Sarma, M. Welch, Dr. F.-J. Zhang  
Department of Chemical Synthesis, Roche Palo Alto  
3431 Hillview Avenue, Palo Alto, CA 94304 (USA)

[g] P. Inbar, Dr. D. Stefanidis  
Department of Discovery Pharmaceuticals, Roche Palo Alto  
3431 Hillview Avenue, Palo Alto, CA 94304 (USA)

Efavirenz and nevirapine are two non-nucleoside reverse transcriptase inhibitors (NNRTIs) that are commonly used as part of first-line therapy in patients that have not previously

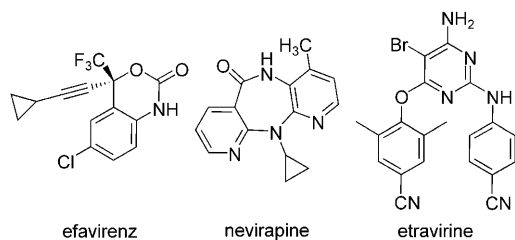


Figure 1. Selected approved NNRTIs.

been exposed to antiretroviral medicines (Figure 1). These medicines are fairly well tolerated, although central nervous system effects, hepatotoxicity, and rash can occur. Both drugs circulate at very high levels, and the efficacy and durability of combination antiretroviral treatment with efavirenz, in particular, has not been surpassed in clinical trials comparing this compound with other agents.<sup>[5,6,7]</sup> When patients that are treated with efavirenz or nevirapine do experience viral breakthrough, the mutant virus K103N is often observed.<sup>[8]</sup> This mutant virus is resistant to both medicines and is produced by a single point mutation. As a consequence of this inherently facile route to resistance development, efavirenz and nevirapine are considered to have a low genetic barrier to resistance. Other NNRTI-resistant viruses commonly observed in patients that experience viral breakthrough include the Y181C and G190A strains.<sup>[9]</sup>

There have been many efforts to discover NNRTIs that suppress the replication of viruses resistant to current NNRTIs and that have a higher genetic barrier to resistance.<sup>[10,11]</sup> The NNRTI etravirine (Figure 1) was recently found to be efficacious for the treatment of patients that had previously been shown to carry virus resistant to efavirenz or nevirapine.<sup>[12]</sup> High-level resistance to etravirine requires at least two mutations of the viral genome. Other compounds that are reported to have a higher genetic barrier to resistance than efavirenz are currently being studied in clinical trials with treatment-naïve patients.<sup>[13,14]</sup> It remains to be determined whether any of these medicines have the pharmacokinetic features required for superior treatment durability.

We previously reported the discovery of a series of diaryl ethers that inhibit common NNRTI-resistant mutant viruses.<sup>[15]</sup> These compounds have good oral bioavailability and long half-lives in multiple animal species. The diaryl ether NNRTIs feature

a functionality that engages in one or more hydrogen bonding interactions with the backbone amide of K103. This portion of the inhibitor strongly influences both the activity against resistant mutant enzymes and inhibitor bioavailability. Herein we focus on the discovery and synthesis of a number of new diaryl ether inhibitors that exhibit strong antiviral activity and favorable pharmacokinetics in animals.

## Chemistry

The HIV reverse transcriptase (RT) inhibitors 1–14 described herein are shown in Figure 2. The synthesis of each of these compounds commenced with the preparation of diaryl ether 15, which was obtained in good yield from a nucleophilic aro-

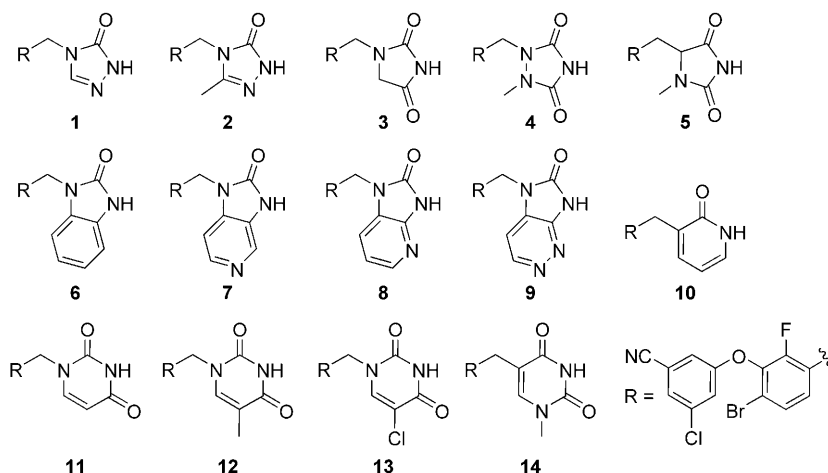
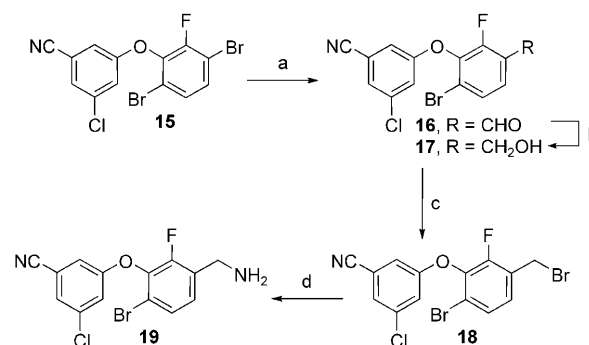


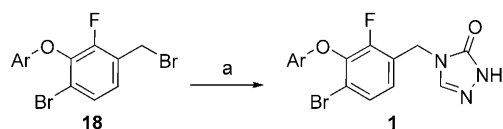
Figure 2. Diaryl ether NNRTIs.

matic substitution reaction between 1,4-dibromo-2,3-difluorobenzene and 3-chloro-5-cyanophenol. Regioselective halogen-metal exchange<sup>[16]</sup> and quenching with *N,N*-dimethylformamide provided aldehyde 16, which was converted into key intermediates 18 and 19 using standard procedures (Scheme 1). Triazolones 1, 2, and 4, imidazolones 6 and 8, and uracil analogues 11–13 were prepared by alkylation of the corre-



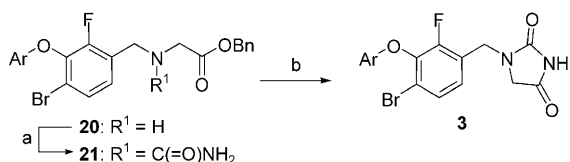
Scheme 1. Synthesis of intermediates 16–19: a) *i*PrMgCl, THF, then DMF,  $-78 \rightarrow 22^\circ\text{C}$ ; b) NaBH<sub>4</sub>, MeOH, THF,  $22^\circ\text{C}$ ; c) PBr<sub>3</sub>, CH<sub>2</sub>Cl<sub>2</sub>,  $22^\circ\text{C}$ , or MsCl, NEt<sub>3</sub>, CH<sub>2</sub>Cl<sub>2</sub>,  $22^\circ\text{C}$ , then LiBr, THF,  $80^\circ\text{C}$ ; d) potassium isoindole-1,3-dione, DMF,  $50^\circ\text{C}$ , then N<sub>2</sub>H<sub>4</sub>, THF, EtOH,  $80^\circ\text{C}$ , or HMTA, EtOH,  $70^\circ\text{C}$ .

spending heterocycle with benzyl bromide **18**, as exemplified by the synthesis of triazolone **1** in Scheme 2.

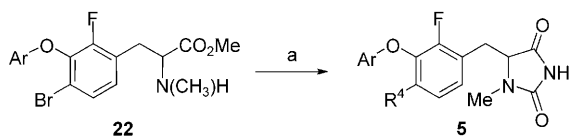


**Scheme 2.** Synthesis of triazolone **1**: a) 2,4-dihydro[1,2,4]triazol-3-one, KI, K<sub>2</sub>CO<sub>3</sub>, CH<sub>3</sub>CN, 85 °C. Ar = 3-chloro-5-cyanophenyl.

A reductive amination reaction between aldehyde **16** and glycine benzyl ester provided amino acid ester **20**. This compound was treated with trimethylsilylisocyanate to form urea **21** (Scheme 3). Base-promoted cyclization of **21** gave hydantoin **3**. Similarly, amino acid ester **22** was obtained from alkylation of **18** with sarcosine methyl ester, which was transformed into racemic hydantoin **5** (Scheme 4).

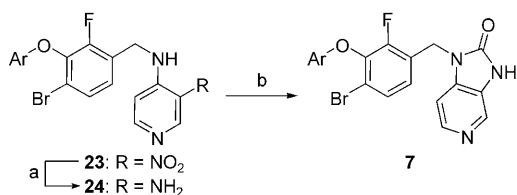


**Scheme 3.** Synthesis of hydantoin **3**: a) trimethylsilylisocyanate, DMAP, THF, 50 °C; b) NaH, DMF, 22 °C. Ar = 3-chloro-5-cyanophenyl.

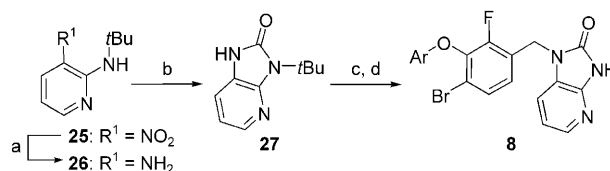


**Scheme 4.** Synthesis of hydantoin **5**: a) trimethylsilylisocyanate, DMAP, THF, 50 °C; Ar = 3-chloro-5-cyanophenyl.

The synthesis of imidazopyridinone **7** began with amine **23**, which was prepared in good yield from the reaction of benzyl amine **19** with 4-chloro-3-nitropyridine. Reduction of the nitro group to the amine with iron and acylation with 1,1-carbonyldiimidazole (CDI) produced the desired inhibitor **7** (Scheme 5). The preparation of isomeric imidazopyridinone **8** is outlined in Scheme 6. Protected intermediate **27** was generated by reduction of nitropyridine **25** and cyclization with CDI. Alkylation of

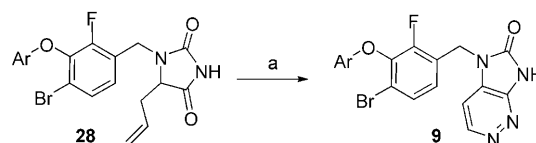


**Scheme 5.** Synthesis of imidazopyridinone **7**: a) Fe, NH<sub>4</sub>Cl, EtOH, H<sub>2</sub>O, 100 °C, or Fe, AcOH, HCl, 70 °C; b) CDI, DMF, 50 °C or CDI, NEt<sub>3</sub>, CH<sub>3</sub>CN, 22 °C. Ar = 3-chloro-5-cyanophenyl.



**Scheme 6.** Synthesis of imidazopyridinone **8**: a) 10% Pd/C, MeOH, H<sub>2</sub>, 22 °C; b) CDI, CH<sub>3</sub>CN, 50 °C; c) NaH, DMF, 22 °C. d) TFA, MsOH, 75 °C. Ar = 3-chloro-5-cyanophenyl.

this heterocycle with **18** and deprotection under strongly acidic conditions gave the desired inhibitor in moderate yield. Allylated hydantoin **28** could be procured in two steps from aldehyde **16**, following procedures similar to those described for the production of **3**. Oxidative cleavage<sup>[17]</sup> of the olefin with OsO<sub>4</sub>/NaIO<sub>4</sub> provided an intermediate aldehyde that reacted with hydrazine and spontaneously oxidized in situ to produce imidazopyridazinone **9** (Scheme 7). Carbon-linked uracil **14**, the isomer of inhibitor **12**, was prepared by desulfurization and alkylation of thiouracil intermediate **30** (Scheme 8). This intermediate was derived from malonate **29** in a three-step sequence that involved decarboxylation, formylation, and cyclization with thiourea.



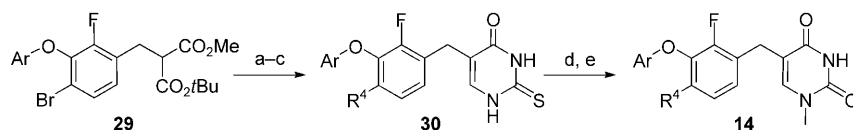
**Scheme 7.** Synthesis of imidazopyridinone **9**: a) OsO<sub>4</sub>, NaIO<sub>4</sub>, H<sub>2</sub>O, THF, 22 °C, then N<sub>2</sub>H<sub>4</sub>, AcOH. Ar = 3-chloro-5-cyanophenyl.

## Molecular Modeling

Modeling was performed with structural information derived from in-house and published structures of NNRTI-RT complexes. These data provide considerable insight into the movements induced in the binding site upon binding of the NNRTIs. The open NNRTI binding pocket of recently reported pyridazinone inhibitors<sup>[15]</sup> was selected for modeling inhibitors presented herein. Molecules were modeled using the molecular mechanics program Moloc.<sup>[18]</sup> Ligand molecules were optimized in the protein environment using the MAB force field and 500 steps of conjugate gradient. No constraints were placed on the ligand atoms during minimization. Similarly, no constraints were placed on the movement of protein residues that display significant positional variability in NNRTI-RT structures. Binding modes were captured in the manuscript using the program PyMOL.<sup>[19]</sup>

## Results

Compounds prepared in this study were screened for inhibition of the RNA-directed DNA polymerase activity of HIV RT using both the wild-type enzyme and an engineered K103N/



**Scheme 8.** Synthesis of uracil **14**: a) TFA,  $\text{CH}_2\text{Cl}_2$ ,  $22^\circ\text{C}$ ; b)  $t\text{BuOK}$ , ethyl formate,  $\text{Et}_2\text{O}$ ,  $22^\circ\text{C}$ ; c) thiourea,  $i\text{PrOH}$ ,  $80^\circ\text{C}$ ; d) chloroacetic acid, acetic acid,  $100^\circ\text{C}$ , then  $\text{H}_2\text{O}$ ,  $22^\circ\text{C}$ ; e)  $N,O$ -bis(trimethylsilyl)acetamide,  $\text{CH}_2\text{Cl}_2$ ,  $22^\circ\text{C}$ , then  $\text{CH}_3\text{I}$ ,  $30^\circ\text{C}$ . Ar = 3-chloro-5-cyanophenyl.

Y181C mutant polymerase. The inhibitors were also studied for their ability to prevent infection-induced cell death in HIV-infected T lymphoblastoid (MT4) cells using both K103N/Y181C and wild-type virus. The K103N/Y181C mutant is resistant to inhibition by efavirenz and nevirapine, and has previously been highlighted as a key target of next-generation NNRTIs.<sup>[20]</sup> Data from the polymerase and antiviral assays are listed in Table 1.

Carbon-linked triazolinone compounds that have excellent pharmacokinetic profiles and good antiviral activity recently reported.<sup>[15]</sup> These compounds interact with the protein backbone of the viral reverse transcriptase through the N/NH hydrogen bond acceptor/donor pair of the triazolinone ring. The nitrogen-linked triazolinone **1** was initially prepared to determine if compounds designed to interact with the protein backbone through the carbonyl group and the acidic nitrogen atom of the triazolinone ring would maintain the activity of their isomeric analogues. Although **1** showed good activity against the K103N/Y181C polymerase, its antiviral activity was modest. Modeling indicated that a small hydrophobic substituent at the 5-position of the triazolinone would be accommodated; however, the addition of a methyl group at this position (compound **2**) did not improve potency in the cellular antiviral assay. Somewhat more potent inhibitors were obtained with

other five-membered heterocycles, and nitrogen-linked hydantoin **3** and urazole **4** were potent inhibitors of the wild-type virus in the polymerase and cell-based assays. The chiral hydantoin **5** was found to be the most potent inhibitor of the mutant polymerase in this series, and separation of the constituent enantiomers provided compound **5a**, which inhibited viral reproduction for the wild-type and mutant enzymes at single-digit nanomolar concentrations. The opposite enantiomer was determined to be more than 50-fold less active, and modeling studies suggest that the more potent enantiomer **5a** is likely to be the *S* sense of inhibitor **5** (Figure 3).

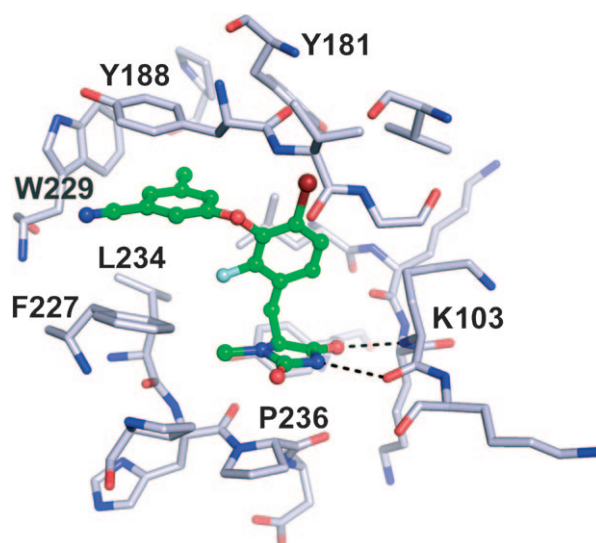


**Figure 3.** Binding mode of compound **5a** modeled in the NNRTI binding pocket.

Imidazolinone **6** displays good potency, and the addition of a nitrogen atom in the phenyl ring as in imidazopyridinone **7** provided a compound that was active at sub-nanomolar concentrations in the wild-type antiviral assay. Analogues **8** and **9**, which contain a pyridine nitrogen in the 4-position of the phenyl ring, were not strong inhibitors of polymerase activity in the cellular assay, although they were equipotent inhibitors of wild-type and mutant polymerase activity.

Carbon- and nitrogen-linked uracils were the most potent NNRTIs in the series of six-membered heterocycles that were examined. Addition of a methyl (compound **12**) or chloro (compound **13**) substituent at the 5-position of the uracil improved the ability of the inhibitors to decrease replication of the K103N/Y181C mutant virus in the antiviral assay.

To develop an understanding of the structure–activity relationships of compounds in this series, inhibitors **6** and **12** were modeled in the NNRTI binding pocket (Figure 4). The terminal ring of the inhibitors is located in a hydrophobic pocket de-

**Table 1.** RT inhibition and antiviral potency of diaryl ether compounds.

Compound <sup>[a]</sup>	$\text{IC}_{50\text{ WT}}$ [nM] <sup>[b]</sup>	$\text{IC}_{50\text{ K103N/Y181C}}$ [nM] <sup>[c]</sup>	$\text{EC}_{50\text{ WT}}$ [nM] <sup>[d]</sup>	$\text{EC}_{50\text{ K103N/Y181C}}$ [nM] <sup>[e]</sup>
nevirapine	1500	> 100 000	80	NT <sup>[g]</sup>
efavirenz	3	94	2	83
<b>1</b>	45	13	14	55
<b>2</b>	55	12	11	> 100
<b>3</b>	9	11	4	> 100
<b>4</b>	7	5	3	28
<b>5</b>	6	7	4	11
<i>ent</i> - <b>5</b> <sup>[f]</sup>	2	2	1	4
<b>6</b>	13	8	5	46
<b>7</b>	5	4	0.4	6
<b>8</b>	6	5	3	20
<b>9</b>	5	4	4	38
<b>10</b>	19	18	25	> 100
<b>11</b>	4	4	1	19
<b>12</b>	3	3	1	11
<b>13</b>	4	4	2	10
<b>14</b>	6	NT	5	66

[a] See Figure 1 for compound structures. [b] Inhibition of RNA-dependent DNA polymerase activity using the wild-type polymerase. [c] Inhibition of RNA-dependent DNA polymerase activity using the K103N/Y181C polymerase. [d] Antiviral activity in MT4 cells using wild-type virus. [e] Antiviral activity in MT4 cells using the K103N/Y181C virus. [f] The more potent enantiomer of compound **5**. [g] NT = not tested.



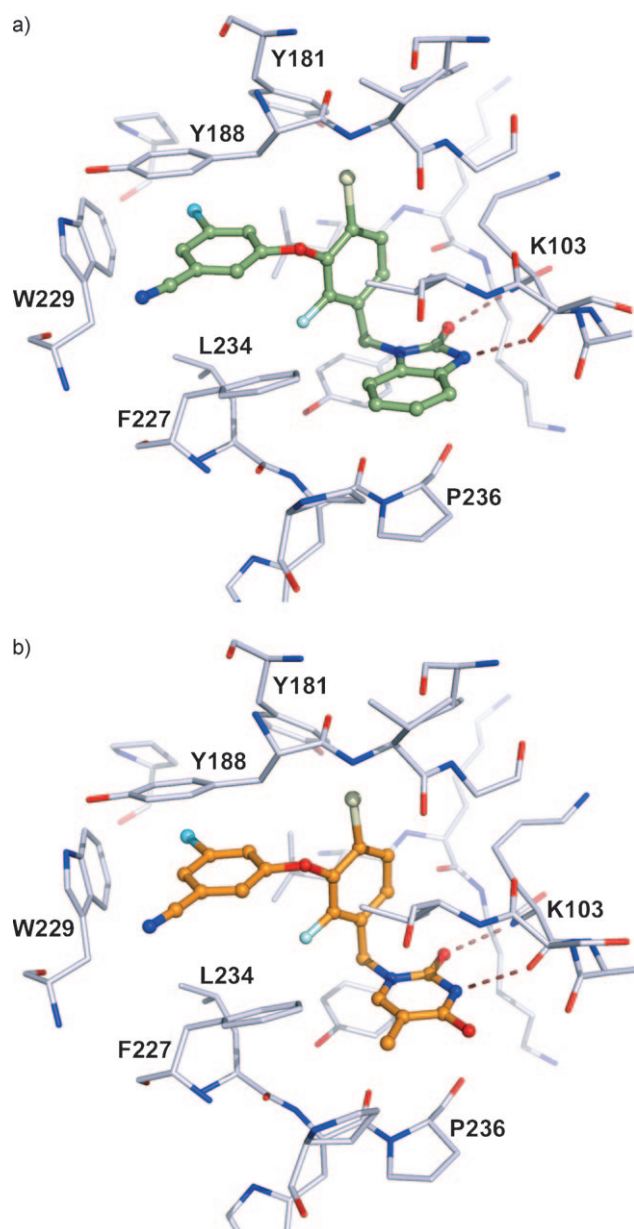


**Figure 4.** Compounds a) **6** (light green) and b) **12** (orange) modeled in the NNRTI binding pocket.

finer by F227, W229, L234, and Y188. Particularly noticeable are edge-to-face interactions with W229, a residue that is highly conserved and is required for efficient viral replication.<sup>[21]</sup> The Y181 residue, which is generally found oriented

toward W299 in structures of NNRTIs complexed with the polymerase,<sup>[22]</sup> was modeled to sit in the same rotamer that is found in X-ray crystal structures of the unliganded enzyme with other diaryl ether NNRTIs. The thymidine ring of **12** makes bidentate hydrogen bond interactions with the K103 backbone amide, and the flexible loops containing residues F227–P225 and P236–L237 are positioned in the open conformation found in structures of the polymerase with delavirdine<sup>[23]</sup> and capravirine.<sup>[24]</sup> The methyl group of the thymidine occupies a small pocket near F227 and P236, and engages in hydrophobic contacts with P225. The unoccupied carbonyl group of the ring extends toward the solvent/enzyme interface. The benzimidazolinone ring of **6** engages in similar donor/acceptor interactions with the K103 amide of the polymerase. In this case, the phenyl group of the benzimidazolinone occupies much of the same volume as the methyl group of inhibitor **12**, and the accessibility of the solvent opening provides clear opportunity for the hydrophilic nitrogen atoms of inhibitors **7–9** to be accommodated.

Compounds **7** and **12**, which had excellent potency in the antiviral assays, were selected for further antiviral profiling and pharmacokinetic study in rat and dog. Thymine compound **12**, displayed low to moderate clearance in rat and very low clearance in dog (Table 2). Although reasonable exposures were obtained following oral dosing, the bioavailability ( $F\%$ ) when the compound was administered as an aqueous suspension was only 10%. Imidazopyridone **7**, which had substantially improved solubility [solubility of **7** (pH 5):  $57 \mu\text{g mL}^{-1}$ ; solubility of **12** (pH 5):  $< 1 \mu\text{g mL}^{-1}$ ] also had good stability in vivo, and the bioavailability of this compound in dog was calculated to be 70%.

The ability of compounds **7** and **12** to inhibit NNRTI-resistant viruses was further assessed in testing against a panel of NNRTI-resistant clinical isolates (Table 3). These viruses were selected based on their decreased susceptibility to efavirenz, and the diversity of viral isolates was chosen to represent the majority of NNRTI resistance patterns that have been described in clinical practice. Compounds **7** and **12** strongly inhibited a majority of the highly NNRTI-resistant viruses in this panel, including all viruses that contain the prevalent K103 mutation.

## Discussion

All of the inhibitors described herein were designed to interact with the backbone amide residue of K103 in a bidentate fashion. For each heterocycle, a carbonyl moiety was presumed to serve as a hydrogen bond acceptor for the K103 amide NH,

**Table 2.** Pharmacokinetic studies of NNRTIs **7** and **12** in rat and dog.<sup>[a]</sup>

Compound	CL [ $\text{mL min}^{-1} \text{kg}^{-1}$ ] <sup>[c]</sup>	Rat <sup>[b]</sup>			Dog <sup>[b]</sup>			AUC [ $\mu\text{M}\cdot\text{h}$ ]
		$V_{d\text{ss}}$ [ $\text{L kg}^{-1}$ ]	$t_{1/2}$ [h]	AUC [ $\mu\text{M}\cdot\text{h}$ ]	$V_{d\text{ss}}$ [ $\text{L kg}^{-1}$ ]	$t_{1/2}$ [h]	AUC [ $\mu\text{M}\cdot\text{h}$ ]	
<b>7</b>	22	5.2	6.2	0.84	3.0	1.4	5.6	13.8
<b>12</b>	10	8.3	11.4	2.54	1.7	1.6	12.4	8.73

[a] See Figure 1 for compound structures. [b] Rat and dog dosed intravenously at  $0.5 \text{ mg kg}^{-1}$  and orally as a suspension at  $2 \text{ mg kg}^{-1}$ ; AUC: 0–24 h; see experimental section for details. [c] CL = clearance.

**Table 3.** Potency of efavirenz, **7**, and **12** against a panel of NNRTI-resistant clinical isolates.

Virus <sup>[a]</sup>	EFV <sup>[b]</sup>	IC <sub>50</sub> [nM]		NNRTI-Associated Mutations <sup>[c]</sup>
		<b>7</b>	<b>12</b>	
CNDO	2	1	1	–
<b>6</b>	> 500	1	2	L100, K103
<b>12</b>	> 500	1	2	L100, K103
<b>14</b>	237	17	11	A98, K103, V108, M230
<b>16</b>	170	2	2	K103, P225
<b>17</b>	160	3	4	A98, K103, Y181
<b>20</b>	53	2	2	K103, Y181
<b>21</b>	35	2	2	K103, V179, Y181
<b>29</b>	36	1	1	K103, Y181
<b>31</b>	24	3	3	A98, V179, Y181
<b>32</b>	16	8	5	V106, V179, Y181, G190
<b>43</b>	132	6	8	K103, Y181, P225

[a] EC<sub>50</sub> (nM) in Monogram Biosciences PhenoScreen™ single-cycle antiviral assay. [b] EFV = efavirenz. [c] Mutations listed in this column do not include NRTI mutations identified in the clinical isolates.

while the acidic NH was placed to interact with the carbonyl unit of the same residue. Delavirdine, a marketed NNRTI, engages in similar interactions with the K103 backbone through a 2-ketoindole unit,<sup>[25]</sup> and a number of recently reported compounds employ an aryl amide as a hydrogen bond acceptor with the amide NH of this residue.<sup>[26]</sup> Capravirine and similar compounds also engage in hydrogen bonding interactions with K103.<sup>[27]</sup> Importantly, as K103 is located adjacent to the solvent opening of the hydrophobic NNRTI pocket, polar functionality is tolerated in this region. The hydrophobicity of the rest of the NNRTI binding pocket requires that these hydrophilic residues modulate the lipophilicity and solubility of the antiviral agents.

While the backbone amide unit of K103 and the solvent channel are occupied by hydrophilic portions of the second-generation NNRTIs, the flexible loop region on the opposite side of this strand is bordered by hydrophobic phenylalanine, proline, and leucine residues (L234, F227, P234). V106 and P236 further define this area. Examination of the models of compounds **6** and **12** in the NNRTI binding pocket reveals that the central phenyl ring of both inhibitors engages in hydrophobic interactions with the methylene units of K103 and the aromatic ring of Y181. These favorable contacts are not present when the inhibitor binds the K103N/Y181C mutant. Extensive modification of the heterocyclic portion of the diphenyl ether inhibitors and optimization of the interactions with residues that line the flexible loops has allowed us to identify NNRTIs that maintain potency against the K103N/Y181C mutant virus, despite the loss of the hydrophobic contacts that exist in the wild-type enzyme. It is interesting to note that the structural modifications that affect potency against the K103N/Y181C mutant are remote from both the 103 and 181 residues. The 5-methyluracil group of **12** makes hydrophobic interactions with F227 and P225, and comparison of the ability of the inhibitors **11–13** (which contain H, CH<sub>3</sub>, or Cl at this position) to block replication of the wild-type and mutant virus in the antiviral assay reveals that while appropriate substitution of the uracil

heterocycle does not appreciably affect the wild-type potency of the inhibitors, these modifications do affect the activity against the K103N/Y181C mutant.

The position of the central and terminal phenyl rings of the imidazolinone compound **6** and uracil **12** are only slightly shifted by the different vectors imposed by the five-membered imidazolinone and six-membered uracil rings. The six-membered portion of the imidazolinone ring of **6** also makes hydrophobic contacts with F227 and P225 and has close contact with the C $\beta$  atom of V106 and the backbone carbon atom of P236. These contacts should be maintained for the clinically observed NNRTI mutant viruses V106A and P236L, and analogue **7** potently inhibits replication of both of these NNRTI-resistant strains (EC<sub>50</sub> (V106A): 2 nM, EC<sub>50</sub> (P236L): 1 nM). The C4 and C5 atoms of the benzimidazolinone ring are adjacent to the solvent opening, and both imidazopyridones **7** and **8**, which have nitrogen atoms at this position, were found to be potent inhibitors of the wild-type and NNRTI-resistant viruses.

## Conclusions

Combination antiretroviral therapy with non-nucleoside reverse transcriptase inhibitors has been demonstrated to provide an excellent treatment option for patients infected with HIV. NNRTIs currently administered to treatment-naïve patients have very long half-lives and maintain consistently high concentrations of the drug in plasma.<sup>[28]</sup> Efforts to improve the genetic barrier to resistance of these agents has led to the identification of many compounds that have a large hydrophobic surface area and contacts that are distributed amongst many different residues in the hydrophobic NNRTI binding pocket. These inhibitors often have low solubility in aqueous solution.

Herein we describe new diaryl ether NNRTIs that are active against wild-type HIV and key NNRTI-resistant mutant viruses. Modeling studies of complexes of two of these inhibitors with HIV reverse transcriptase demonstrate that the compounds make hydrophobic contacts with a number of residues in the NNRTI binding pocket. This feature may contribute to the resilience of these inhibitors against NNRTI-resistant mutations. Antiviral agents **7** and **12** have promising pharmacokinetic profiles. Compound **12** has excellent stability and exhibits reasonable exposure in both rat and dog, but the bioavailability following oral administration of an aqueous suspension appears to be solubility-limited. Imidazopyridinone **7**, which contains a moderately basic nitrogen atom, maintains acceptable stability in vivo and has improved bioavailability. Advanced studies with other diphenyl ether NNRTIs will be described in future reports.

## Experimental Section

### Chemistry

**General:** Column chromatography was performed on Analogix or Isco automatic chromatography instruments using pre-packed silica gel columns. ESIMS data were recorded with a Finnegan LCQ spectrometer equipped with Excalibur. <sup>1</sup>H NMR spectra were recorded at room temperature in the indicated solvent on a Bruker

300, 400, or 500 MHz spectrometer. Chemical shifts ( $\delta$ ) are given in ppm. Microanalyses of solid compounds were carried out with an Exeter CE-440 analyzer. High-resolution ESIMS data were recorded on a Waters LCT instrument equipped with Masslynx. Purchased chemicals were used as obtained without purification. Unless otherwise specified, all chemical transformations were performed under nitrogen atmosphere in anhydrous solvents that were purchased from Aldrich or EMD.

**3-Chloro-5-(3,6-dibromo-2-fluorophenoxy)benzotrile (15):** NaH (0.042 g of a 60% dispersion in mineral oil, 1.05 mmol) was added to a solution of 3-chloro-5-hydroxybenzotrile (0.15 g, 1 mmol) and *N,N*-dimethylacetamide (DMA, 1 mL), and the resulting mixture was stirred at 50 °C for 30 min. 1,4-Dibromo-2,3-difluorobenzene was added to the solution (2.7 g, 10 mmol), and the resulting mixture was heated at 125 °C for 2 h. The solution was cooled and diluted with EtOAc and washed with an equal volume of 10% H<sub>2</sub>SO<sub>4</sub>. The organic extracts were dried (MgSO<sub>4</sub>), filtered and concentrated. The crude product was purified by silica gel chromatography, eluting with EtOAc/hexanes (10% v/v) to afford biaryl ether **15** (331 mg, 82%). <sup>1</sup>H NMR (300 MHz, CDCl<sub>3</sub>):  $\delta$  = 7.43–7.38 (m, 3H), 7.16 (m, 1H), 7.01 (m, 1H).

**3-(6-Bromo-2-fluoro-3-formylphenoxy)-5-chlorobenzotrile (16):** *i*PrMgCl (3.08 mL of a 2 M solution in THF, 6.16 mmol) was added to a solution of **15** (2.00 g, 4.93 mL) in toluene (40 mL) maintained under an Ar atmosphere and cooled to –78 °C. The solution was stirred for 1 h, and a solution of CuCN·2LiCl (1 M in THF, 0.1 mL) was added. The resulting mixture was stirred at –50 °C for 2 h, and the reaction mixture was then transferred via cannula into a flask containing DMF (0.57 mL, 7.4 mmol) and toluene (10 mL) which was maintained at –78 °C. The combined solution was warmed to 22 °C and quenched by the addition of saturated aqueous NH<sub>4</sub>Cl. The organic phase was separated, washed with brine, dried (MgSO<sub>4</sub>), and evaporated to dryness under reduced pressure to afford aldehyde **16** (1.50 g, 86%) as an off-white solid. <sup>1</sup>H NMR (300 MHz, CDCl<sub>3</sub>):  $\delta$  = 10.30 (d, *J* = 0.7 Hz, 1H), 7.74 (dd, *J* = 6.4 Hz, 8.5 Hz, 1H), 7.63 (m, 1H), 7.40 (dd, *J* = 1.3 Hz, 1.8 Hz, 1H), 7.18 (t, *J* = 2.0 Hz, 1H), 7.05 (m, 1H).

**3-(6-Bromo-2-fluoro-3-hydroxymethylphenoxy)-5-chlorobenzotrile (17):** NaBH<sub>4</sub> (0.128 g, 3.38 mmol) was added in portions to a stirred solution of the aldehyde (0.80 g, 2.25 mmol) in THF (5 mL) and MeOH (5 mL) at 22 °C. After stirring for 24 h, the reaction mixture was quenched by the addition of saturated aqueous NH<sub>4</sub>Cl. The organics were extracted with EtOAc, washed with brine, dried (MgSO<sub>4</sub>), and evaporated to dryness under reduced pressure. Silica gel chromatography (EtOAc/hexanes 10→50% v/v) provided alcohol **17** (0.25 g, 31%). <sup>1</sup>H NMR (300 MHz, CDCl<sub>3</sub>):  $\delta$  = 7.74 (dd, *J* = 1.7 Hz, 8.4 Hz, 1H), 7.32–7.37 (m, 2H), 7.15 (dd, 1H, *J* = 1.9 Hz, 2.2 Hz, 1H), 6.99–7.03 (m, 1H), 4.77 (s, 2H).

**3-(6-Bromo-3-bromomethyl-2-fluorophenoxy)-5-chlorobenzotrile (18):** *Method 1:* PBr<sub>3</sub> (9.3 mL, 1.0 M in CH<sub>2</sub>Cl<sub>2</sub>) was added to a stirred solution of **17** (3.00 g, 8.41 mmol) in CH<sub>2</sub>Cl<sub>2</sub> (100 mL). The reaction mixture was stirred at 22 °C for 24 h and quenched by the addition of saturated aqueous NaHCO<sub>3</sub>. The organic phase was separated, washed with brine, dried (MgSO<sub>4</sub>), and evaporated to dryness under reduced pressure. The product was purified by silica gel chromatography, eluting with a gradient of EtOAc/hexanes (20→50% v/v EtOAc) to afford **18** as white crystals (2.0 g, 57%). *Method 2:* Compound **17** (71.2 g, 0.20 mol) was dissolved in CH<sub>2</sub>Cl<sub>2</sub> (500 mL) and cooled to 0 °C. Triethylamine (50.2 mL, 0.36 mol) and then methanesulfonyl chloride (34.4 g, 0.30 mol) were added slowly, keeping the temperature below 4 °C. The mixture was

stirred at 2–5 °C for 1.5 h, then quenched with cold 2 M H<sub>2</sub>SO<sub>4</sub> (200 mL) (temperature: 8–10 °C). The phases were separated, and the aqueous phase was extracted with CH<sub>2</sub>Cl<sub>2</sub>. The combined organic phase was washed with saturated aqueous KBr (200 mL). The organic phase was dried over Na<sub>2</sub>SO<sub>4</sub> and concentrated under reduced pressure to afford the mesylate as a reddish oil. The mesylate (85.4 g, 197 mmol) was dissolved in 400 mL THF. LiBr (34.8 g, 400 mmol) was added, and the mixture was stirred at ambient temperature overnight and then held at reflux for 2 h. The suspension was filtered to remove the solid, and the filtrate was evaporated to dryness. The residue was suspended in CH<sub>2</sub>Cl<sub>2</sub> and filtered through silica gel (100 g). The CH<sub>2</sub>Cl<sub>2</sub> solvent was replaced with *i*PrOH (200 mL) to precipitate the product as yellowish solid, which was isolated by filtration and dried under vacuum (53.3 g). A second crop (7.7 g) was obtained by recrystallizing the mother liquor contents from *i*PrOH (73% combined yield). <sup>1</sup>H NMR (300 MHz, CDCl<sub>3</sub>):  $\delta$  = 7.47 (dd, *J* = 8.7 Hz, 1.9 Hz, 1H), 7.37 (m, 1H), 7.28 (m, 1H), 7.16 (m, 1H), 7.00 (m, 1H), 4.48 (s, 2H).

**3-(3-Aminomethyl-6-bromo-2-fluorophenoxy)-5-chlorobenzotrile (19):** *Method 1:* The potassium salt of isoindole-1,3-dione (10.5 g, 57.2 mmol) was added to a solution of **18** (21.6 g, 52 mmol) in DMF (200 mL), and the solution was stirred at 50 °C for 16 h. Solid precipitated out of solution after a short period. The reaction was cooled to 22 °C, poured into 300 mL H<sub>2</sub>O, and filtered. The solid was washed with a small amount of Et<sub>2</sub>O and dried under vacuum to afford 3-[6-bromo-3-(1,3-dioxo-1,3-dihydroisoindol-2-ylmethyl)-2-fluorophenoxy]-5-chlorobenzotrile (20 g, 80% yield). Hydrazine (1.62 mL, 50 mmol) was added slowly to a suspension of the imide (5.0 g, 10 mmol) in a mixture of THF (80 mL) and EtOH (20 mL). The solution was slowly heated to 80 °C, and the reaction mixture became homogenous. After 1 h, most of the solvent was removed, and the residue was partitioned between EtOAc/hexanes and H<sub>2</sub>O. The organic layer was washed with aqueous NaHCO<sub>3</sub>, and the organic layer was again evaporated to dryness under reduced pressure. The product was purified by silica gel chromatography, eluting with a CH<sub>2</sub>Cl<sub>2</sub>/(60:10:1 CH<sub>2</sub>Cl<sub>2</sub>/MeOH/NH<sub>4</sub>OH) gradient (0→30% of a CH<sub>2</sub>Cl<sub>2</sub>/MeOH/NH<sub>4</sub>OH solution) to afford the primary amine **19** (1.25 g, 34%). *Method 2:* A suspension of **18** (8.38 g, 20 mmol) and hexamethylenetetramine (HMTA) (3.36 g, 24 mmol) in EtOH (80 mL) was stirred at 70 °C for 4 h. H<sub>2</sub>O (64 mL) was added, and the mixture was stirred at 70 °C for 0.5 h. The mixture was cooled to 45 °C. HCl (5 M, 16 mL) was added, and the reaction temperature was maintained at 45 °C for 1 h. The organic solvent was removed under reduced pressure. The suspension was cooled with ice. The solid was filtered, washed with 1 M HCl, and dried at 50 °C under vacuum. The salt of the desired amine (**19**-HX; X = Br, Cl) was obtained as a mixture of hydrochloride and hydrobromide salts as an off-white solid (8.08 g). <sup>1</sup>H NMR (300 MHz, CDCl<sub>3</sub>):  $\delta$  = 7.45 (dd, *J* = 8.5 Hz, 1.7 Hz, 1H), 7.35 (m, 1H), 7.28 (m, 1H), 7.15 (t, *J* = 2.3 Hz, 1H), 7.0 (m, 1H), 3.94 (s, 2H), 1.55 (s, 2H).

**3-[6-Bromo-2-fluoro-3-(5-oxo-1,5-dihydro[1,2,4]triazol-4-ylmethyl)phenoxy]-5-chlorobenzotrile (1):** A solution of **18** (200 mg, 0.48 mmol), 2,4-dihydro[1,2,4]triazol-3-one (0.040 g, 0.48 mmol), K<sub>2</sub>CO<sub>3</sub> (0.13 g, 0.96 mmol), and KI (0.008 g, 0.1 mmol) in CH<sub>3</sub>CN (1.5 mL) was heated at 85 °C for 2 h and then cooled to 22 °C. The reaction mixture was diluted with MeOH/CH<sub>2</sub>Cl<sub>2</sub> (10% v/v), and washed sequentially with H<sub>2</sub>O and brine. The organic extracts were evaporated, and the crude product was purified by silica gel chromatography, eluting with a MeOH/CH<sub>2</sub>Cl<sub>2</sub> gradient (3→10% MeOH) to afford **1** as a white solid (0.020 g, 10%). <sup>1</sup>H NMR (300 MHz, CD<sub>3</sub>OD):  $\delta$  = 7.84 (s, 1H), 7.60–7.53 (m, 2H), 7.27–7.21



(m, 3H), 4.94 (s, 2H); MS (ESI): 423  $[M+H]^+$ ; Anal. calcd for  $C_{16}H_9BrClFN_4O_2$ : C 45.36, H 2.14, N 13.23; found: C 45.57, H 2.19, N 13.00.

**3-[6-Bromo-2-fluoro-3-(3-methyl-5-oxo-1,5-dihydro[1,2,4]triazol-4-ylmethyl)phenoxy]-5-chlorobenzonitrile (2)**: Prepared as described for compound **1**, replacing 2,4-dihydro[1,2,4]triazol-3-one with 5-methyl-2,4-dihydro[1,2,4]triazol-3-one. The product was purified by silica gel chromatography, eluting with a MeOH/ $CH_2Cl_2$  gradient (1.5→7% MeOH) to afford **2** (0.020 g, 16%).  $^1H$  NMR (300 MHz,  $CD_3OD$ ):  $\delta$  = 7.59–7.56 (m, 2H), 7.26 (m, 2H), 7.15 (dd,  $J$  = 8.5 Hz, 7.4 Hz, 1H), 4.95 (s, 2H), 2.20 (s, 3H); MS (ESI): 437  $[M+H]^+$ ; Anal. calcd for  $C_{17}H_{11}BrClFN_4O_2$ : C 46.65, H 2.53, N 12.80; found: C 46.37, H 2.58, N 12.51.

**[4-Bromo-3-(3-chloro-5-cyanophenoxy)-2-fluorobenzylamino]-acetic acid benzyl ester (20)**: Glycine benzyl ester (925 mg, 5.6 mmol) was dissolved in 1,2-dichloroethane (25 mL), and aldehyde **16** (2.0 g, 5.6 mmol) and  $NaBH(OAc)_3$  (1.66 g, 7.8 mmol) were added sequentially. After stirring overnight, the reaction mixture was quenched with saturated aqueous  $Na_2CO_3$  and extracted with  $Et_2O$ . The organic layers were washed with brine, dried ( $MgSO_4$ ), and concentrated. The product was purified by silica gel chromatography, eluting with an EtOAc/hexanes gradient (20→30% EtOAc) to afford ester **20** (1.60 g, 57%).  $^1H$  NMR (300 MHz,  $CDCl_3$ ):  $\delta$  = 7.43–7.42 (m, 7H), 7.24 (m, 1H), 7.16 (t,  $J$  = 2.2, 1H), 7.01 (m, 1H), 5.16 (s, 2H), 3.87 (s, 2H), 3.48 (s, 2H).

**{1-[4-Bromo-3-(3-chloro-5-cyanophenoxy)-2-fluorobenzyl]-ureido}acetic acid benzyl ester (21)**: Trimethylsilylisocyanate (0.34 mL, 0.25 mmol) and 4-dimethylaminopyridine (DMAP, 12 mg, 0.10 mmol) were added to a solution of **20** (510 mg, 1.01 mmol) and THF (5 mL). The resulting solution was heated at 50 °C for 20 h, cooled to 22 °C, and concentrated. The product was purified by silica gel chromatography, eluting with an EtOAc/hexanes gradient (33→66% EtOAc) to afford **21** (0.28 g, 51%).  $^1H$  NMR (300 MHz,  $CDCl_3$ ):  $\delta$  = 7.42–7.22 (m, 8H), 7.16 (t,  $J$  = 2.2 Hz, 1H), 7.00 (m, 1H), 5.14 (s, 2H), 4.66 (brs, 2H), 4.58 (s, 2H), 4.08 (s, 2H).

**3-[6-Bromo-3-(2,4-dioxoimidazolidin-1-ylmethyl)-2-fluorophenoxy]-5-chlorobenzonitrile (3)**: NaH (20 mg, 60% in mineral oil, 0.52 mmol) was added to a solution of **21** (250 mg, 0.48 mmol) in DMF (3 mL) at 0 °C. The reaction mixture was stirred at 22 °C for 2 h, poured into saturated  $NH_4Cl$  (20 mL), and extracted with EtOAc. The organic layers were washed with brine, dried ( $MgSO_4$ ), and concentrated to afford **3** (0.190 g, 95%).  $^1H$  NMR (300 MHz,  $CDCl_3$ ):  $\delta$  = 8.46 (s, 1H), 7.41 (dd,  $J$  = 8.4 Hz, 1.9 Hz, 1H), 7.37 (m, 1H), 7.23 (dd,  $J$  = 8.4 Hz, 7.0 Hz, 1H), 7.15 (t,  $J$  = 1.9 Hz, 1H), 7.00 (dd,  $J$  = 2.4 Hz, 1.3 Hz, 1H), 4.60 (d,  $J$  = 1.2 Hz, 2H), 3.92 (s, 2H); MS (ESI): 438  $[M+H]^+$ ; Anal. calcd for  $C_{17}H_{10}BrClFN_3O_3$ : C 46.55, H 2.30, N 9.58; found: C 46.62, H 2.23, N 9.48.

**3-[6-Bromo-2-fluoro-3-(2-methyl-3,5-dioxo[1,2,4]triazolidin-1-ylmethyl)phenoxy]-5-chlorobenzonitrile (4)**: A solution of 1-methyl-[1,2,4]triazolidine-3,5-dione (0.021 g, 0.18 mmol) and NaH (0.09 g of a 60% dispersion in oil, 0.21 mmol) in DMSO (1 mL) was stirred at 22 °C for 20 min. Benzyl bromide **18** (0.075 g, 0.18 mmol) was added, and the mixture turned clear and was stirred for 1.5 h. The reaction was quenched with  $H_2O$  and extracted with 10% MeOH/ $CH_2Cl_2$ . The product was purified by silica gel chromatography, eluting with a MeOH/ $CH_2Cl_2$  mixture (0→10% MeOH) to provide material that was purified further by preparative TLC (0.02 g, 25%).  $^1H$  NMR (300 MHz,  $[D_6]DMSO$ ):  $\delta$  = 8.98 (s, 1H), 7.48 (dd,  $J$  = 8.5 Hz, 1.5 Hz, 1H), 7.37 (m, 1H), 7.26 (m, 2H), 7.13 (t,  $J$  = 2.2 Hz, 1H), 7.00 (m, 1H), 4.79 (s, 2H), 3.12 (s, 3H); MS (ESI): 451  $[M-H]$ ; HRMS (ESI)

calcd for  $C_{17}H_{12}BrClFN_4O_3$   $[M+H]^+$ : 454.9738; found: 454.9722; LC purity: 96%.

**3-[4-Bromo-3-(3-chloro-5-cyanophenoxy)-2-fluorophenyl]-2-methylaminopropionic acid methyl ester (22)**: A solution of diisopropylamine (0.14 mL, 1 mmol) in THF was cooled to –78 °C, and *n*-butyllithium (1 mmol of a solution in hexanes) was then added. The reaction mixture was warmed to 0 °C for 15 min. (*tert*-Butoxycarbonylmethylamino)acetic acid methyl ester (0.2 g, 1.2 mmol) was added, and the resulting solution was stirred for 30 min. The mixture was cooled to –78 °C, and a THF solution of **18** (0.35 g, 0.83 mmol) was added. The reaction was warmed to 22 °C and stirred for 4 h, poured into aqueous  $NH_4Cl$ , and extracted with EtOAc. The organic layer was washed with  $H_2O$ , dried ( $Na_2SO_4$ ), and purified by silica gel chromatography to afford 0.2 g of the protected amine. A solution of the carbamate, trifluoroacetic acid (TFA, 1 mL), and  $CH_2Cl_2$  was stirred at 0 °C for 5 h. The organic solvents were evaporated to dryness, and the residue was dissolved in  $CH_2Cl_2$ . The organic layer was washed with saturated  $Na_2CO_3$  and brine, dried ( $Na_2SO_4$ ), and the solvents evaporated to afford **22** (0.15 g, 40%).  $^1H$  NMR (300 MHz,  $CDCl_3$ ):  $\delta$  = 7.40 (dd,  $J$  = 8.3 Hz, 1.9 Hz, 1H), 7.34 (t,  $J$  = 1.5 Hz, 1H), 7.15 (t,  $J$  = 2.3 Hz, 1H), 7.11–7.01 (m, 2H), 3.67 (s, 3H), 3.44 (m, 1H), 3.08–2.89 (m, 2H), 2.37 (s, 3H).

**3-[6-Bromo-2-fluoro-3-methyl-2,5-dioxoimidazolidin-4-ylmethyl)-phenoxy]-5-chlorobenzonitrile (5)**: Trimethylsilylisocyanate (–0.9 mL, 0.58 mmol) was added to a solution of **22** (0.1 g, 0.23 mmol) and DMAP (4 mg, 0.03 mmol) in THF (1 mL), and the reaction mixture was heated at 50 °C for 18 h. The volatile materials were evaporated under reduced pressure, and the residue was dissolved in  $CH_2Cl_2$  and MeOH. The organic layer was washed with saturated  $NaHCO_3$  and then brine. The organic layer was dried ( $Na_2SO_4$ ), and the organic solvents were evaporated. The crude product was purified by preparative TLC to afford **5** (0.030 g, 30%). The enantiomers of this compound could be separated with a Chiralpak IA analytical column, eluting with EtOH/hexanes.  $^1H$  NMR (300 MHz,  $[D_6]DMSO$ ):  $\delta$  = 10.71 (s, 1H), 7.80 (s, 1H), 7.61 (d,  $J$  = 8.3 Hz, 1H), 7.42 (m, 1H), 7.36 (m, 1H), 7.22 (t,  $J$  = 8.0 Hz, 1H), 4.29 (t,  $J$  = 5.2 Hz, 2H), 3.16 (m, 1H), 2.76 (s, 3H); MS (ESI): 452  $[M+H]^+$ ; HRMS (ESI) calcd for  $C_{18}H_{13}BrClFN_3O_3$   $[M+H]^+$ : 453.9786; found: 453.9778; LC purity: 100%.

**3-[6-Bromo-2-fluoro-3-(2-oxo-2,3-dihydrobenzimidazol-1-ylmethyl)phenoxy]-5-chlorobenzonitrile (6)**: A mixture of **18** (0.448 g, 1.07 mmol), 2-hydroxybenzimidazole (0.860 g, 6.41 mmol),  $K_2CO_3$  (0.295 g, 2.13 mmol), and DMF (2 mL) was heated by microwave at 100 °C for 10 min. The reaction mixture was cooled, diluted with EtOAc, washed with brine, dried ( $Na_2SO_4$ ), and evaporated to dryness. The residue was triturated with EtOAc to remove excess 2-hydroxybenzimidazole. The filtrate was evaporated under reduced pressure to afford **6** as an off-white solid (0.180 g, 35%).  $^1H$  NMR (300 MHz,  $[D_6]DMSO$ ):  $\delta$  = 11.01 (s, 1H), 7.81 (m, 1H), 7.60 (m, 1H), 7.49 (m, 1H), 7.44 (m, 1H), 7.11 (m, 1H), 7.00 (m, 4H), 5.08 (s, 2H); MS (ESI): 472  $[M+H]^+$ ; Anal. calcd for  $C_{21}H_{12}BrClFN_3O_2$ : C 53.36, H 2.56, N 8.89; found: C 53.15, H 2.53; N: 8.79.

**3-[6-Bromo-2-fluoro-3-[(3-nitropyridin-4-ylamino)methyl]phenoxy]-5-chlorobenzonitrile (23)**: *Method 1*: 4-Chloro-3-nitropyridine (0.18 g, 0.92 mmol) and  $Na_2CO_3$  (0.188 g, 1.77 mmol) were added to a solution of **19** (0.275 g, 0.77 mmol) in DMA (5 mL). After stirring for 2.5 h at 50 °C the entire reaction mixture was poured into  $H_2O$  (20 mL) and extracted with EtOAc. The organic layers were washed with brine, dried ( $MgSO_4$ ), and concentrated. The product was purified by silica gel chromatography, eluting with an EtOAc/hexane gradient (33→65% EtOAc) to afford 0.28 g



(76%) of **23**. *Method 2*: A solution of the tosylate salt of compound **19** (285 g, 0.55 mol) in 1.4 L *N*-methyl-4-pyrrolidinone (NMP), 285 mL H<sub>2</sub>O, and 310 mL Et<sub>3</sub>N was cooled in an ice bath. 4-Chloro-3-nitropyridine (123 g, 0.77 mol) was added, and the mixture was stirred overnight at room temperature. H<sub>2</sub>O (1140 mL) was added to the slurry over 2.5 h to cause precipitation of the product. The product was isolated by filtration and washed with 2780 mL H<sub>2</sub>O. Amine **23** was obtained as a yellow solid (249 g, 94% yield). <sup>1</sup>H NMR (300 MHz, CDCl<sub>3</sub>): δ = 9.27 (s, 1H), 8.60 (m, 1H), 8.35 (d, *J* = 5.7 Hz, 1H), 7.50 (dd, *J* = 8.3 Hz, 1.9 Hz, 1H), 7.39 (t, *J* = 1.5 Hz, 1H), 7.17 (m, 2H), 7.03 (m, 1H), 6.70 (d, *J* = 6.3 Hz, 1H), 4.66 (d, *J* = 6.0 Hz, 2H).

**3-[3-(3-Aminopyridin-4-ylamino)methyl]-6-bromo-2-fluorophenoxy]-5-chlorobenzonitrile (24)**: *Method 1*: NH<sub>4</sub>Cl (0.124 g, 2.32 mmol), H<sub>2</sub>O (1 mL), and Fe powder (0.13 g, 2.32 mmol) were slowly added to a solution of **23** (0.277 g, 0.58 mmol) in EtOH (3 mL). After heating for 2.5 h at 100 °C, the reaction mixture was cooled to 22 °C, filtered through Celite and concentrated. The crude product was purified by silica gel chromatography, eluting with a MeOH/CH<sub>2</sub>Cl<sub>2</sub> gradient (5→15% MeOH) to afford compound **24** (0.085 g, 33%). *Method 2*: Iron powder (30.7 g, 0.550 mol) was combined with acetic acid (214 mL, 3.4 mol), and the suspension was stirred. Concentrated aqueous HCl (4.5 mL, 0.054 mol) was added, and the slurry was stirred for 25 min and then heated at 60 °C. A solution of **23** (105.0 g, 0.220 mol) in 525 mL NMP was added slowly to the iron-acetic acid mixture, maintaining the reaction temperature below 70 °C. After the addition was complete, the reaction mixture was kept at 70 °C until the completion (8 h). The mixture was cooled to room temperature and diluted with 540 mL H<sub>2</sub>O. The slurry was filtered through Celite, and the Celite pad was washed with 550 mL H<sub>2</sub>O. The combined filtrates were stirred while adding 3 *N* aqueous HCl (100 mL, 0.300 mol) to cause precipitation of the product as a hydrochloride salt. The resulting slurry was filtered, and the product cake was washed with H<sub>2</sub>O and dried under vacuum at ~70 °C to provide **24**·HCl as a colorless solid (87.1 g, 81.8% yield). <sup>1</sup>H NMR (300 MHz, CD<sub>3</sub>OD): δ = 7.76 (dd, *J* = 6.6 Hz, 1.2 Hz, 1H), 7.70 (d, *J* = 1.2, 1H), 7.56 (m, 2H), 7.32 (dd, *J* = 8.5 Hz, 7.3 Hz, 1H), 7.26 (t, *J* = 2.2 Hz, 1H), 7.19 (m, 1H), 6.78 (d, *J* = 6.6 Hz, 1H).

**3-[6-Bromo-2-fluoro-3-(2-oxo-2,3-dihydroimidazo[4,5-*c*]pyridin-1-ylmethyl)phenoxy]-5-chlorobenzonitrile (7)**: *Method 1*: 1,1-Carbonyldiimidazole (34 mg, 0.21 mmol) was added to a solution of **24** (85 mg, 0.19 mmol) in DMF (1 mL). After stirring for 3 days at 50 °C, an additional portion of CDI was added, and the temperature was increased to 100 °C. After 4 h, the reaction mixture was cooled, poured into H<sub>2</sub>O (5 mL), and extracted with EtOAc. The organic layers were then washed with brine, dried (MgSO<sub>4</sub>), and concentrated under reduced pressure. Trituration of the residue with Et<sub>2</sub>O afforded compound **7** (0.060 g, 66%). *Method 2*: A solution of **24**·HCl (280 g, 0.58 mol), 1,1-carbonyldiimidazole (196 g, 1.21 mol), Et<sub>3</sub>N (202 mL), and CH<sub>3</sub>CN (1.7 L) was stirred at room temperature for 1.5 h. H<sub>2</sub>O (600 mL) was added, and the solution was seeded with small amounts of seed crystals of **6**. After stirring overnight at room temperature, additional H<sub>2</sub>O (1.25 L) was added over 2.5 h. The slurry was filtered, and washed with H<sub>2</sub>O (3.7 L). Compound **7** was obtained as an off-white solid (255 g, 93%). <sup>1</sup>H NMR (300 MHz, [D<sub>6</sub>]DMSO): δ = 11.33 (s, 1H), 8.23 (d, *J* = 1 Hz, 1H), 7.07 (d, *J* = 5.3 Hz, 1H), 7.82 (m, 1H), 7.60 (dd, *J* = 8.5 Hz, 1.7 Hz, 1H), 7.51 (m, 1H), 7.45 (m, 1H), 7.15 (dd, *J* = 8.4 Hz, 7.4 Hz, 1H), 7.11 (d, *J* = 5.3 Hz, 1H), 5.12 (s, 2H); MS (ESI): 473 [M+H]<sup>+</sup>; Anal. calcd for C<sub>20</sub>H<sub>11</sub>BrClFN<sub>4</sub>O<sub>2</sub>: C 50.71, H 2.34, N 11.83; found: C 50.49, H 2.34; N: 11.67.

**tert-Butyl-(3-nitropyridin-2-yl)amine (25)**: *tert*-Butylamine (19 mL, 180 mmol) was added to a solution of 2-chloro-3-nitropyridine (9.5 g, 59.9 mmol) and DMF (150 mL). After stirring for 2 days at 45 °C, the reaction mixture was concentrated. The residue was dissolved in Et<sub>2</sub>O (300 mL), and the organic layer was washed with H<sub>2</sub>O and brine, dried (MgSO<sub>4</sub>), filtered, and concentrated to afford **25** (11.6 g, 98%). <sup>1</sup>H NMR (300 MHz, CDCl<sub>3</sub>): δ = 8.39 (m, 2H), 6.59 (m, 1H), 1.55 (s, 9H).

***N*-tert-Butylpyridine-2,3-diamine (26)**: Pd/C (10%, 1 g) was added to a solution of **25** (11.6 g, 59.9 mmol) and MeOH (50 mL). The resulting suspension was stirred under an H<sub>2</sub> atmosphere for 18 h, filtered through Celite, and concentrated. The product was purified by silica gel chromatography, eluting with an EtOAc/hexane gradient (10→50% EtOAc) to afford compound **26** (3.3 g, 33%). <sup>1</sup>H NMR (300 MHz, CDCl<sub>3</sub>): δ = 7.74 (dd, *J* = 5.1 Hz, 1.6 Hz, 1H), 6.81 (dd, *J* = 7.3 Hz, 1.6 Hz, 1H), 6.46 (dd, *J* = 7.3 Hz, 5.1 Hz, 1H), 4.04 (brs, 1H), 3.08 (brs, 2H), 1.48 (s, 9H).

**3-tert-Butyl-1,3-dihydroimidazo[4,5-*b*]pyridin-2-one (27)**: 1,1-Carbonyldiimidazole (4.5 g, 27.4 mmol) was added to a solution of **26** (3.3 g, 21.1 mmol) in CH<sub>3</sub>CN (50 mL), and the reaction mixture was stirred for 2 h at 50 °C. After the reaction was complete, the mixture was concentrated, dissolved in EtOAc (300 mL), washed with H<sub>2</sub>O and brine, dried (MgSO<sub>4</sub>), filtered, and concentrated under reduced pressure. The product was purified by silica gel chromatography, eluting with an EtOAc/hexane gradient (10→50% EtOAc) to afford 2.6 g (64%) of the benzimidazole product. <sup>1</sup>H NMR (300 MHz, CDCl<sub>3</sub>): δ = 8.01 (dd, *J* = 5.2 Hz, 1.6 Hz, 1H), 7.25 (dd, *J* = 7.7 Hz, 1.6 Hz, 1H), 6.94 (dd, *J* = 7.7 Hz, 5.2 Hz, 1H), 1.87 (s, 9H).

**3-[6-Bromo-2-fluoro-3-(2-oxo-2,3-dihydroimidazo[4,5-*b*]pyridin-1-ylmethyl)phenoxy]-5-chlorobenzonitrile (8)**: NaH (0.024 g, 0.59 mmol, 60% mineral oil dispersion) was added to a solution of **27** (0.10 g, 0.52 mmol) in DMF (2 mL) at 0 °C. After stirring for 15 min, **18** (0.199 mg, 0.475 mmol) was added, and stirring was continued at 22 °C for 30 min. The reaction mixture was poured into H<sub>2</sub>O (10 mL) and extracted EtOAc. The organics were washed with brine, dried (MgSO<sub>4</sub>), filtered, and concentrated under reduced pressure. The product was purified by silica gel chromatography, eluting with an EtOAc/hexane gradient (10→30% EtOAc) to afford 0.20 g (72%) of the protected benzimidazolinone. A solution of the imidazolinone (175 mg, 0.33 mmol), TFA (1.3 mL), and MsOH (0.33 mL) was heated at 75 °C for 4 h. The mixture was concentrated, and the residue was dissolved in EtOAc (300 mL), washed with H<sub>2</sub>O and brine, dried (MgSO<sub>4</sub>), filtered, and concentrated. The product was largely the amide resulting from hydrolysis of the nitrile (135 mg, 0.275 mmol). This material was suspended in dioxane (1.4 mL) and successively treated with pyridine (0.20 mL, 2.48 mmol) and trifluoroacetic anhydride (TFAA, 0.112 mL, 0.83 mmol) at 0 °C. The mixture was then gently warmed to 60 °C for 5 h. The solution was poured into 20 mL H<sub>2</sub>O, and extracted with EtOAc. The organic layers were washed with brine, dried (MgSO<sub>4</sub>), concentrated, and triturated with Et<sub>2</sub>O to afford **8** (0.025 g, 11%). <sup>1</sup>H NMR (300 MHz, [D<sub>6</sub>]DMSO): δ = 11.70 (s, 1H), 7.93 (dd, *J* = 5.3 Hz, 1.3 Hz, 1H), 7.81 (m, 1H), 7.60 (dd, *J* = 8.4 Hz, 1.8 Hz, 1H), 7.50 (m, 1H), 7.45 (m, 1H), 7.32 (dd, *J* = 7.7 Hz, 1.1 Hz, 1H), 7.18 (dd, *J* = 8.3 Hz, 7.5 Hz, 1H), 6.99 (dd, *J* = 7.8 Hz, 5.2 Hz, 1H), 5.11 (s, 2H); MS (ESI): 473 [M+H]<sup>+</sup>; Anal. calcd for C<sub>20</sub>H<sub>11</sub>BrClFN<sub>4</sub>O<sub>2</sub>: C 50.71, H 2.34, N 11.83; found: C 50.72, H 2.41, N 11.43.

**3-[3-(5-Allyl-2,4-dioximidazolidin-1-ylmethyl)-6-bromo-2-fluorophenoxy]-5-chlorobenzonitrile (28)**: Allylglycine methyl ester (0.73 g, 5.6 mmol of free base that was formed from treatment of the hydrochloride salt in Et<sub>2</sub>O with saturated Na<sub>2</sub>CO<sub>3</sub>) was dissolved

in 1,2-dichloroethane (25 mL), and **16** (2.0 g, 5.6 mmol) followed by NaBH(OAc)<sub>3</sub> (1.66 g, 7.84 mmol) were added. The reaction mixture was stirred overnight, quenched with saturated Na<sub>2</sub>CO<sub>3</sub>, and extracted with Et<sub>2</sub>O. The organics were washed with brine, dried (MgSO<sub>4</sub>), filtered, and concentrated. The product was purified by silica gel chromatography, eluting with an EtOAc/hexane gradient (20→30% EtOAc) to afford 1.25 g (48%) of the desired ester. Trimethylsilylisocyanate (1.0 mL, 2.5 equiv) and DMAP (32 mg, 0.10 equiv) were added to a solution of the ester (1.20 g, 2.60 mmol) in THF (13 mL). This solution was heated at 50 °C for 3 days, cooled, and concentrated. The product was purified by silica gel chromatography, eluting with an EtOAc/hexane gradient (33→66% EtOAc) to afford 1.11 g (88%) of the hydantoin **28**. <sup>1</sup>H NMR (300 MHz, CDCl<sub>3</sub>): δ = 8.50 (brs, 1 H), 7.50 (dd, *J* = 8.4 Hz, 1.8 Hz, 1 H), 7.38 (t, *J* = 1.6 Hz, 1 H), 7.27 (dd, *J* = 8.4 Hz, 7.1 Hz, 1 H), 7.13 (t, *J* = 2.2 Hz, 1 H), 7.01 (m, 1 H), 5.60 (m, 1 H), 5.19 (m, 2 H), 4.87 (dd, *J* = 15.8 Hz, 1.6 Hz, 1 H), 4.33 (d, *J* = 15.8 Hz, 1 H), 3.99 (t, *J* = 4.64 Hz, 1 H), 2.66 (m, 2 H).

**3-[6-Bromo-2-fluoro-3-(6-oxo-6,7-dihydroimidazo[4,5-c]pyridazin-5-ylmethyl)phenoxy]-5-chlorobenzonitrile (9)**: OsO<sub>4</sub> (0.100 mL, 5% in *tert*-BuOH) followed by a solution of NaIO<sub>4</sub> (1.36 g, 6.39 mmol) in H<sub>2</sub>O (2.8 mL) was added to a solution of **28** (1.02 g, 2.13 mmol) in THF (8.5 mL). The thick mixture was stirred for 24 h, diluted with saturated aqueous NaHCO<sub>3</sub>, and extracted with EtOAc. The organic layers were washed with brine, dried (MgSO<sub>4</sub>), filtered, and concentrated to provide the corresponding aldehyde. The aldehyde was dissolved in AcOH (17 mL), and hydrazine (0.670 mL, 21.3 mmol) was added. After stirring for an additional 24 h, the mixture was concentrated and purified by silica gel chromatography, eluting with a MeOH/CH<sub>2</sub>Cl<sub>2</sub> gradient (1→7% MeOH) to afford a solid that was further purified by reversed-phase HPLC (0.010 g, 1%). <sup>1</sup>H NMR (300 MHz, CD<sub>3</sub>OD): δ = 8.70 (d, *J* = 5.3 Hz, 1 H), 7.81 (m, 1 H), 7.60 (dd, *J* = 8.5 Hz, 1.7 Hz, 1 H), 7.50 (m, 1 H), 7.45 (m, 1 H), 7.22 (m, 1 H), 7.18 (d, *J* = 5.3 Hz, 1 H), 5.10 (s, 2 H); MS (ESI): 474 [M+H]<sup>+</sup>; HRMS (ESI) calcd for C<sub>19</sub>H<sub>11</sub>BrClFN<sub>5</sub>O<sub>2</sub> [M+H]<sup>+</sup>: 473.9763; found: 473.9750. LC purity: 100%.

**3-[6-Bromo-2-fluoro-3-(2-oxo-1,2-dihydropyridin-3-ylmethyl)phenoxy]-5-chlorobenzonitrile (10)**: *n*-Butyllithium (0.91 mL, 1.4 M in hexanes) was added slowly to a cooled (−78 °C) solution of 3-bromo-2-methoxypyridine (0.225 g, 1.2 mmol) in dry THF (3 mL). The mixture was stirred for 10 min and then CuI (0.141 mg, 0.74 mmol) was added. After 30 min, the mixture was warmed to 0 °C and stirred for 20 min. The material was cooled to −40 °C for 45 min, and then cooled back down to −78 °C. A solution of **18** (0.316 mg, 0.9 mmol) in THF (2.5 mL) was added dropwise. After 5 min, the cooling bath was removed and the mixture was warmed to ambient temperature, stirred for 5 h, and added to a saturated aqueous solution of NH<sub>4</sub>Cl. The mixture was extracted with EtOAc, and the organic phase was collected and washed with brine. The aqueous phases were extracted with EtOAc and the combined organic phases were dried (MgSO<sub>4</sub>) and evaporated to dryness under reduced pressure. Purification by preparative TLC (silica, eluting with 16% EtOAc/hexanes) provided the desired methoxypyridine as a light yellow semi-solid (250 mg). This material and NaI (168 mg, 1.1 mmol) were dissolved in dry CH<sub>3</sub>CN (40 mL) and stirred at 0 °C. Chlorotrimethylsilane (0.14 mL, 1.12 mmol) was added dropwise, and the mixture was warmed to 22 °C and stirred for 16 h. NaI (0.168 g, 1.1 mmol) was added, and the solution was cooled to 0 °C. Additional TMSCl (0.14 mL, 1.12 mmol) was added, and the mixture was stirred at 22 °C for 8 h. 1 N HCl (0.5 mL) was added followed by 38% aqueous sodium bisulfite, brine, H<sub>2</sub>O, and EtOAc, and the mixture was stirred for 30 min. The phases were

separated, and the aqueous phase was extracted with EtOAc. The organic solution was stirred with NaHCO<sub>3</sub> (200 mg) and a solution of 38% sodium metabisulfite (1 mL) in H<sub>2</sub>O (40 mL) for 15 min. The organic phase was collected and washed with brine, and the aqueous phases were extracted with EtOAc. The organic phases were combined, dried (MgSO<sub>4</sub>), and filtered, and the volatile materials were removed. Purification by preparative TLC (silica, eluting with 75% EtOAc/hexanes) followed by crystallization from hot CH<sub>2</sub>Cl<sub>2</sub>/hexanes provided **10** (0.124 g, 32%). <sup>1</sup>H NMR (300 MHz, CDCl<sub>3</sub>): δ = 12.30 (s, 1 H), 7.39 (dd, *J* = 8.5 Hz, 1.5 Hz, 1 H), 7.34 (m, 1 H), 7.31–7.18 (m, 3 H), 7.15 (t, *J* = 2.0 Hz, 1 H), 7.00 (m, 1 H), 6.83 (t, *J* = 6.7 Hz, 1 H), 3.90 (s, 2 H); MS (ESI): 433 [M+H]<sup>+</sup>; Anal. calcd for C<sub>19</sub>H<sub>11</sub>BrClFN<sub>2</sub>O<sub>2</sub>·0.25 H<sub>2</sub>O: C 52.08, H 2.65, N 6.39; found: C 52.08, H 2.47, N 6.39.

**3-[6-Bromo-3-(2,4-dioxo-3,4-dihydro-2H-pyrimidin-1-ylmethyl)-2-fluorophenoxy]-5-chlorobenzonitrile (11)**: A solution of **18** (0.12 g, 0.286 mmol), TMSCl (2 drops), hexamethyldisilazane (0.3 mL), 1,2-dichloroethane (2 mL), iodine (~5 mg), and uracil (0.16 g, 1.43 mmol) were combined under nitrogen and stirred for 18 h at 80 °C. The reaction was cooled, the organics evaporated under reduced pressure, and the residue dissolved in CH<sub>2</sub>Cl<sub>2</sub> and washed with H<sub>2</sub>O. The organic solution was dried (MgSO<sub>4</sub>), filtered and evaporated. The crude product was purified by silica gel chromatography, eluting with a MeOH/CH<sub>2</sub>Cl<sub>2</sub> gradient (1→7% MeOH) to afford 0.07 g (55%) of **11**. <sup>1</sup>H NMR (300 MHz, [D<sub>6</sub>]DMSO): δ = 10.00 (s, 1 H), 7.62–7.55 (m, 3 H), 7.32 (m, 3 H), 5.55 (d, *J* = 8.1 Hz, 1 H), 4.99 (s, 2 H); MS (ESI): 450 [M+H]<sup>+</sup>; Anal. calcd for C<sub>18</sub>H<sub>10</sub>BrClFN<sub>3</sub>O<sub>3</sub>: C 47.97, H 2.24, N 9.32; found: C 47.88, H 2.19, N 9.27.

**3-[6-Bromo-2-fluoro-3-(5-methyl-2,4-dioxo-3,4-dihydro-2H-pyrimidin-1-ylmethyl)phenoxy]-5-chlorobenzonitrile (12)**: Prepared as described for compound **11**, replacing uracil with thymine. Compound **12** was purified by silica gel chromatography, eluting with a MeOH/CH<sub>2</sub>Cl<sub>2</sub> gradient (1→6% MeOH) to afford a 90% yield of the desired product. <sup>1</sup>H NMR (300 MHz, [D<sub>6</sub>]DMSO): δ = 11.36 (s, 1 H), 7.81 (t, *J* = 1.5 Hz, 1 H), 7.54–7.45 (m, 4 H), 7.22 (m, 1 H), 4.91 (s, 2 H), 1.76 (d, *J* = 1 Hz, 3 H); MS (ESI): 464 [M+H]<sup>+</sup>; Anal. calcd for C<sub>19</sub>H<sub>12</sub>BrClFN<sub>3</sub>O<sub>3</sub>: C 49.11, H 2.50, N 9.04; found: C 49.06, H 2.53, N 8.76.

**3-[6-Bromo-3-(5-chloro-2,4-dioxo-3,4-dihydro-2H-pyrimidin-1-ylmethyl)-2-fluorophenoxy]-5-chlorobenzonitrile (13)**: Prepared as described for compound **11**, except uracil was replaced with 5-chloro-1H-pyrimidine-2,4-dione. The compound was purified by silica gel chromatography, eluting with a MeOH/CH<sub>2</sub>Cl<sub>2</sub> gradient (1→7% MeOH) to afford **13** in 36% yield. <sup>1</sup>H NMR (300 MHz, [D<sub>6</sub>]DMSO): δ = 11.86 (s, 1 H), 8.22 (s, 1 H), 7.82 (t, *J* = 1.4 Hz, 1 H), 7.62 (dd, *J* = 8.5 Hz, 1.7 Hz, 1 H), 7.52 (m, 1 H), 7.46 (m, 1 H), 7.27 (t, *J* = 7.5 Hz, 1 H), 4.95 (s, 2 H); MS (ESI): 484 [M+H]<sup>+</sup>; Anal. calcd for C<sub>18</sub>H<sub>9</sub>BrCl<sub>2</sub>FN<sub>3</sub>O<sub>3</sub>: C 44.57, H 1.87, N 8.66; found: C 44.43, H 1.78, N 8.71.

**2-[4-Bromo-3-(3-chloro-5-cyanophenoxy)-2-fluorobenzyl]malonic acid *tert*-butyl ester ethyl ester (29)**: *tert*-Butyl ethyl malonate (0.28 g, 1.48 mmol) was added to a suspension of NaH (0.14 g, 3.57 mmol) and DMF (3 mL) and cooled to 0 °C. The mixture was warmed to 22 °C and stirred for 30 min. To the resulting solution was added **18** (0.50 g, 1.19 mmol). The reaction was stirred at 22 °C for 1.5 h and diluted with EtOAc and washed sequentially with saturated NH<sub>4</sub>Cl, H<sub>2</sub>O, and brine. The organic layer was dried (Na<sub>2</sub>SO<sub>4</sub>), filtered, and evaporated under reduced pressure to afford **29** (0.62 g, 99%). <sup>1</sup>H NMR (300 MHz, CDCl<sub>3</sub>): δ = 7.40–7.34 (m, 2 H), 7.14–6.99 (m, 3 H), 4.24–4.09 (m, 3 H), 3.20 (m, 2 H), 1.41 (s, 9 H), 1.12 (m, 3 H).

**3-[6-Bromo-2-fluoro-3-(4-oxo-2-thioxo-1,2,3,4-tetrahydropyrimidin-5-ylmethyl)phenoxy]-5-chlorobenzonitrile (30):** TFA (2 mL) was added to a solution of **29** (0.62 g, 1.18 mmol) and CH<sub>2</sub>Cl<sub>2</sub> (2.5 mL) cooled to 0 °C, and the reaction was warmed to 22 °C. After 6 h, the volatile materials were removed under reduced pressure, the residue diluted with CH<sub>2</sub>Cl<sub>2</sub>, and the organic layer washed sequentially with aqueous NaHCO<sub>3</sub>, H<sub>2</sub>O, and brine. The aqueous wash was acidified with HCl and extracted with CH<sub>2</sub>Cl<sub>2</sub>. The combined organic layers were washed with H<sub>2</sub>O, dried (Na<sub>2</sub>SO<sub>4</sub>), filtered, and evaporated. The residue was dissolved in DMF (2 mL) and H<sub>2</sub>O (0.07 mL) and heated by microwave for 20 min at 160 °C. The reaction mixture was diluted with EtOAc and washed sequentially with H<sub>2</sub>O and brine. The organic layer was dried (Na<sub>2</sub>SO<sub>4</sub>), filtered, and evaporated. The crude product was purified by silica gel chromatography, eluting with an EtOAc/hexanes gradient (0–30% EtOAc) to afford 0.180 g (38%) of the decarboxylated ethyl ester. A solution of this material (0.18 g, 0.42 mmol) and ethyl formate (0.07 mL, 0.92 mmol) in Et<sub>2</sub>O (1 mL) was added dropwise to a solution of *t*BuOK in Et<sub>2</sub>O (2.5 mL). The reaction mixture was warmed to 22 °C and stirred for 18 h. The volatiles were removed in vacuo, and the residue was dissolved in *i*PrOH (5 mL). Thiourea (0.062 g, 0.84 mmol) was added, and the reaction mixture was heated at 80 °C for 4 h. The volatile materials were removed, and the residue was washed with Et<sub>2</sub>O. The residue was dissolved in H<sub>2</sub>O, and the solution was acidified with AcOH. The resulting precipitate was filtered and washed with H<sub>2</sub>O. The residue was dissolved in Et<sub>2</sub>O, and the organic layer was washed with H<sub>2</sub>O and brine. Evaporation of the volatile materials under reduced pressure afforded a small amount of slightly impure **30** (0.1 g, 50%); MS (ESI): 468 [M+H]<sup>+</sup>.

**3-[6-Bromo-2-fluoro-3-(1-methyl-2,4-dioxo-1,2,3,4-tetrahydropyrimidin-5-ylmethyl)phenoxy]-5-chlorobenzonitrile (14):** Chloroacetic acid (1 mL) was added to a solution of thioracil **30** (0.1 g, 0.21 mmol). AcOH (1 mL) was added. The reaction mixture was heated at 100 °C for 6 h, cooled to 0 °C, and H<sub>2</sub>O (2 mL) was added. The resulting precipitate was filtered and washed with H<sub>2</sub>O and Et<sub>2</sub>O to afford 0.030 g (31%) of the uracil. *N,O*-bis(trimethylsilyl)acetamide (0.1 mL) was added slowly to a solution of this material in CH<sub>2</sub>Cl<sub>2</sub> (0.9 mL) at 22 °C and stirred for 2 h. CH<sub>3</sub>I (0.145 mL) was added, and the reaction was heated at 28 °C for 18 h. The volatile materials were removed, and the organic residue was dissolved in EtOAc. The organic layer was washed with H<sub>2</sub>O and then brine, dried (Na<sub>2</sub>SO<sub>4</sub>), filtered, and evaporated under reduced pressure. The crude product was purified by silica gel chromatography, eluting with a MeOH/CH<sub>2</sub>Cl<sub>2</sub> gradient (0–4% MeOH) to afford 0.015 g (48%) of **14**. <sup>1</sup>H NMR (300 MHz, CD<sub>3</sub>OD): δ = 7.54 (m, 1H), 7.49–7.45 (m, 2H), 7.25–7.19 (m, 3H), 3.66 (s, 2H), 3.33 (s, 3H); MS (ESI): 464 [M+H]<sup>+</sup>; HRMS (ESI) calcd for C<sub>19</sub>H<sub>13</sub>BrClFN<sub>3</sub>O<sub>3</sub> [M+H]<sup>+</sup>: 465.97729; found: 465.97864; LC purity: 96%.

### Biological methods

**HIV-1 reverse transcriptase assay.** RNA-dependent DNA polymerase activity was measured using a biotinylated primer oligonucleotide and tritiated dNTP substrate. Newly synthesized DNA was quantified by capturing the biotinylated primer molecules on streptavidin (SA)-coated scintillation proximity assay (SPA) beads (Amersham). The sequences of the polymerase assay substrates were: 18-nt DNA primer, 5'-biotin-GTC CCT GTT CGG GCG CCA-3'; 47-nt RNA template, 5'-GGG UCU CUC UGG UUA GAC CAC UCU AGC AGU GGC GCC CGA ACA GGG AC-3'. The biotinylated DNA primer was obtained from Integrated DNA Technologies Inc., and the RNA template was synthesized by Dharmacon. The DNA polymerase assay (final volume 50 μL) contained 32 nm biotinylated

DNA primer, 64 nM RNA substrate, dGTP, dCTP, dTTP (each at 5 μM), 103 nM [<sup>3</sup>H]dATP (specific activity: 29 μCi mmol<sup>-1</sup>) in 45 mM Tris-HCl (pH 8.0), 45 mM NaCl, 2.7 mM Mg(CH<sub>3</sub>COO)<sub>2</sub>, 0.045% Triton X-100 w/v, and 0.9 mM EDTA. The reactions contained 5 μL of serial compound dilutions in 100% DMSO for IC<sub>50</sub> determination, and the final concentration of DMSO was 10%. Reactions were initiated by the addition of 30 μL of the HIV RT enzyme (final concentrations of 1–3 nM). Protein concentrations were adjusted to provide linear product formation for at least 30 min of incubation. After incubation at 30 °C for 30 min, the reaction was quenched by the addition of 50 μL 200 mM EDTA (pH 8.0) and 2 mg mL<sup>-1</sup> SA-PVT SPA beads (Amersham, RPNQ0009, reconstituted in 20 mM Tris-HCl (pH 8.0), 100 mM EDTA, and 1% BSA). The beads were left to settle overnight, and the SPA signals were counted in a 96-well top counter-NXT instrument (Packard). IC<sub>50</sub> values were obtained by sigmoidal regression analysis using GraphPad software.

**Antiviral assay.** Anti-HIV antiviral activity was assessed using an adaptation of the method of Pauwels et al.<sup>[29]</sup> The method is based on the ability of compounds to protect HIV-infected T lymphoblastoid (MT4) cells from cell death mediated by the infection. The endpoint of the assay was calculated as the compound concentration at which viability of the cell culture was preserved by 50% (50% inhibitory concentration, IC<sub>50</sub>). Cell viability was determined by the uptake of soluble, yellow 3-[4,5-dimethylthiazol-2-yl]-2,5-diphenyltetrazolium bromide (MTT) and its reduction to a purple insoluble formazan salt. After solubilization, spectrophotometric methods were employed to measure the amount of formazan product.

MT4 cells were prepared to be in logarithmic-phase growth, with a total of 2 × 10<sup>6</sup> cells infected with the HXB2 strain of HIV at a multiplicity of 0.0001 infectious units per cell in a total volume of 200–500 μL. The cells were incubated with virus for 1 h at 37 °C before removal of virus. The cells were then washed in 0.01 M phosphate-buffered saline (PBS, pH 7.2) before resuspension in culture medium for incubation in culture with serial dilutions of test compound. The culture medium used was RPMI 1640 without phenol red (Gibco, cat# 11835055), supplemented with 10% fetal bovine serum (FBS, Invitrogen, cat# 16000-036), 1% (v/v) penicillin/streptomycin (Invitrogen, cat# 15140-122), and 2 mM L-glutamine (Invitrogen, cat# 25030-081). Test compounds were prepared as 2 mM solutions in dimethyl sulfoxide (DMSO). Four replicate, twofold serial dilutions in GM10 were then prepared, and 50 μL volumes were placed in 96-well plates over a final concentration range of 625–1.22 nM. GM10 (50 μL) and 3.5 × 10<sup>4</sup> infected cells were then added to each well. Control cultures containing no cells (blank), uninfected cells (100% viability; four replicates), and infected cells without compound (total virus-mediated cell death; four replicates) were also prepared. The cultures were then incubated at 37 °C in a humidified atmosphere of 5% CO<sub>2</sub> in air for 5 days. A fresh solution of MTT (5 mg mL<sup>-1</sup>) was prepared in 0.01 M PBS (pH 7.2) and 20 μL were added to each culture. The cultures were further incubated as before for 2 h. They were then mixed by pipetting up and down, 170 μL Triton X-100 in acidified *i*PrOH (10% v/v Triton X-100 in a 1:250 mixture of concentrated HCl/*i*PrOH) was added. When the formazan deposit was fully solubilized by further mixing, the absorbance (OD) of the cultures was measured at λ = 540 nm and λ = 690 nm (readings at 690 nm were used as blanks for artifacts between wells). The percent protection for each treated culture was then calculated from the equation:

$$\% \text{ Protection} = \frac{(\text{OD}_{\text{drug-treated cultures}}) - (\text{OD}_{\text{untreated virus control cultures}})}{(\text{OD}_{\text{uninfected cultures}}) - (\text{OD}_{\text{untreated virus control cultures}})} \times 100$$



The IC<sub>50</sub> values can be obtained from graph plots of percent protection versus log<sub>10</sub> (drug concentration).

**Antiviral assay using clinical isolates.** Viruses were selected from a panel of clinical isolates available at Monogram Biosciences based on their decreased susceptibility to efavirenz. Compounds were evaluated in the PhenoScreen™ single-cycle antiviral assay at Monogram Biosciences as described previously.<sup>[30]</sup>

**Animal experimental protocol:** In vivo experiments were conducted according to IACUC protocol number 2004–44.

**Keywords:** antiviral agents · HIV · inhibitors · molecular modeling · reverse transcriptase · structure-based design

- [1] C. Flexner, *Nat. Rev. Drug Discovery* **2007**, *6*, 959–966.
- [2] V. Von Wyl, S. Yerly, J. Boni, P. Burgisser, T. Klimkait, M. Battegay, H. Furrer, A. Telenti, B. Hirschel, P. L. Vernazza, E. Bernasconi, M. Rickenbach, L. Perrin, B. Ledergerber, H. F. Gunthard, *Arch. Intern. Med.* **2007**, *167*, 1782–1790.
- [3] M. Boffito, D. J. Back, T. F. Blaschke, M. Rowland, R. J. Bertz, J. G. Gerber, V. Miller, *Aids Res. Hum. Retroviruses* **2003**, *19*, 825–835.
- [4] F. V. Leth, B. S. Kappelhoff, D. Johnson, M. H. Losso, A. Boron-Kaczmariska, M. S. Saag, J. M. Livrozet, D. B. Hall, J. Leith, A. D. Huitema, F. W. Wit, *AIDS Res. Hum. Retroviruses* **2006**, *22*, 232–239.
- [5] S. M. Vrouenraets, F. W. Wit, J. van Tongeren, J. M. Lange, *Expert Opin. Pharmacother.* **2008**, *8*, 851–871.
- [6] Z. Zhang, R. Hamatake, Z. Hong, *Antiviral Chem. Chemother.* **2004**, *15*, 121–134.
- [7] L. Waters, L. John, M. Nelson, *Int. J. Clin. Pract.* **2007**, *61*, 105–118.
- [8] M. A. Wainberg, *J. Acquir. Immune Defic. Syndr.* **2003**, *34*(Suppl. 1), S2–S7.
- [9] V. A. Johnson, F. Brun-Vezinet, B. Clotet, B. Conway, R. T. D'Aquila, L. M. Demeter, D. R. Kuritzkes, D. Pillay, J. M. Schapiro, A. Telenti, D. D. Richman, International AIDS Society–USA Drug Resistance Mutations Group, *Top. HIV Med.* **2003**, *11*, 215–221.
- [10] L. R. Boone, *Curr. Opin. Invest. Drugs* **2006**, *7*, 128–135.
- [11] E. De Clercq, *Chem. Biodiversity* **2004**, *1*, 44–64.
- [12] K. Andries, H. Azijn, T. Thielemans, D. Ludovici, M. Kukla, J. Heeres, P. A. J. Janssen, B. De Corte, J. Vingerhoets, R. Pauwels, M.-P. De Bethune, *Antimicrob. Agents Chemother.* **2004**, *48*, 4680–4686.
- [13] F. Goebel, A. Yakovlev, A. L. Pozniak, E. Vinogradova, G. Boogaerts, R. Hoetelmans, M.-P. P. de Bethune, M. Peeters, B. Woodfall, *AIDS* **2006**, *20*, 1721–1726.
- [14] Z. K. Sweeney, K. Klumpp, *Curr. Opin. Drug Discov. Development* **2008**, *11*, 458–470.
- [15] a) Z. K. Sweeney, S. Acharya, A. Briggs, J. P. Dunn, T. R. Elworthy, J. Fretland, A. M. Giannetti, *Bioorg. Med. Chem. Lett.* **2008**, *18*, 4348–4351; b) Z. K. Sweeney, J. P. Dunn, Y. Li, G. Heilek, P. Dunten, T. R. Elworthy, *Bioorg. Med. Chem. Lett.* **2008**, *18*, 4352–4354.
- [16] P. Knochel, W. Dohle, N. Gommermann, F. Kneisel, F. Kopp, T. Korn, I. Sapountzis, V. Vu, *Angew. Chem.* **2003**, *115*, 4438–4456; *Angew. Chem. Int. Ed.* **2003**, *42*, 4302–4320.
- [17] R. Pappo, D. Allen, R. U. Lemieux, W. S. Johnson, *J. Org. Chem.* **1956**, *21*, 478–481.
- [18] P. R. Gerber, K. Muller, *J. Comput. Aided Mol. Design* **1995**, *9*, 251–268.
- [19] W. L. Delano, The PyMOL Molecular Graphics System (2002), <http://www.pymol.org> (access October 26, 2008).
- [20] K. Das, S. G. Sarafianos, A. D. Clark Jr., P. L. Boyer, S. H. Hughes, E. Arnold, *J. Mol. Biol.* **2007**, *365*, 77–89.
- [21] A. L. Hopkins, J. Ren, J. Milton, R. J. Hazen, J. H. Chan, D. I. Stuart, D. K. Stammers, *J. Med. Chem.* **2004**, *47*, 5912–5922.
- [22] A. Beyer, L. Lawtrakul, P. Pungpo, P. Wolschann, *Curr. Comp.-Aided Drug Design* **2007**, *3*, 87–100.
- [23] PDB code 1KLM.
- [24] PDB code 1EP4.
- [25] R. M. Esnouf, J. Ren, A. L. Hopkins, C. K. Ross, E. Y. Jones, D. Stammers, D. Stuart, *Proc. Natl. Acad. Sci. USA* **1997**, *94*, 3984–3989.
- [26] For example, see: T. Jiang, K. L. Kuhlen, K. Wolff, H. Yin, K. Bieza, J. Caldwell, B. Bursulaya, T. Tuntland, K. Zhang, D. Karanewsky, Y. He, *Bioorg. Med. Chem. Lett.* **2006**, *16*, 2109–2112.
- [27] J. Ren, C. Nichols, L. E. Bird, T. Fujiwara, H. Sugimoto, D. I. Stuart, D. K. Stammers, *J. Biol. Chem.* **2000**, *275*, 14316–14320.
- [28] P. F. Smith, R. DiCenzo, G. D. Morse, *Clin. Pharmacokinet.* **2001**, *40*, 893–905.
- [29] R. W. Pauwels, J. Balzarini, M. Baba, R. Snoeck, D. Schols, P. Herdewijn, J. Desmyter, E. De Clercq, *J. Virol. Methods* **1988**, *20*, 309–321.
- [30] C. J. Petropoulos, N. T. Parkin, K. L. Limoli, Y. S. Lie, T. Wrin, W. Huang, H. Tian, D. Smith, G. A. Winslow, D. J. Capon, J. M. Whitcomb, *Antimicrob. Agents Chemother.* **2000**, *44*, 920–928.

Received: August 3, 2008

Revised: September 20, 2008

Published online on November 12, 2008